THE ASTROPHYSICAL JOURNAL, 560:L99–L103, 2001 October 10

GAS-PHASE INFRARED SPECTRUM OF THE CORONENE CATION

JOS OOMENS,[1] BORIS G. SARTAKOV,[1,2] A. G. G. M. TIELENS,[3]
GERARD MEIJER,[1,4] AND GERT VON HELDEN[1]
Received 2001 July 6; accepted 2001 September 4; published 2001 September 20

ABSTRACT

The gas-phase infrared spectrum of the coronene cation in the 700–1700 cm^{-1} range is presented. The spectrum is obtained via multiphoton dissociation spectroscopy of ionic coronene stored in a quadrupole ion trap using the intense and narrowband infrared radiation of a free electron laser. The spectrum shows main absorption peaks at 849, 1327, and 1533 cm^{-1} along with some weak and barely resolved features, in good agreement with density functional calculations if the effects of vibrational anharmonicity are accounted for. Relative line intensities show remarkable differences with respect to matrix isolation data. The novel experimental technique applied here leads in a natural way to an absorption spectrum of highly excited species. Hence, measured absorption spectra can be compared rather directly to interstellar emission spectra, negating to some extent the need for detailed model calculations.

Subject headings: infrared: ISM — ISM: molecules — methods: laboratory — techniques: spectroscopic

Polycyclic aromatic hydrocarbons (PAHs) form an important class of molecules in interstellar chemistry, as they are suggested to be precursors of biogenic molecules that hold the key to the origin of life on Earth (Bernstein et al. 1999). Gas-phase PAHs are believed to be ubiquitously present throughout space and to be the carriers of the unidentified infrared (UIR) emission bands (Leger & Puget 1984; Allamandola, Tielens, & Barker 1985, 1989). After the absorption of a UV photon, internal conversion and intramolecular vibrational redistribution (IVR) occur so that a highly statistical ensemble of vibrational states becomes populated (Allamandola et al. 1989). The extremely low densities in the interstellar medium (ISM) give rise to a negligible collision rate, and thus the molecules release their energy mainly by infrared fluorescence. The wavelengths at which the UIR emission bands are observed roughly match the general CH and CC bending and stretching modes in PAHs, and relative intensities point particularly to ionized PAHs (DeFrees et al. 1993). In fact, the degree of ionization depends on several factors, such as UV photon density, hydrogen density, electron density, and temperature (Salama et al. 1996; Joblin et al. 1996; Sloan et al. 1999), and can amount up to 100%.

Despite the fact that the PAH hypothesis was launched more than 15 years ago, thus far no individual PAH has been identified in the ISM, which is in part due to the limited availability of laboratory spectra for comparison. Nonetheless, it should be noted that neutral benzene was discovered in the proto–planetary nebula CRL 618 very recently (Cernicharo et al. 2001). Substantial progress in the understanding of the spectroscopy of ionic PAHs has been achieved via matrix isolation techniques (Szczepanski et al. 1992; Hudgins, Sandford, & Allamandola 1994; Hudgins & Allamandola 1999a, 1999b), in which the neutral PAH is isolated in a cryogenic rare gas matrix and subsequently ionized by exposure to UV light. The low ionization efficiency causes the subsequently recorded spectra to be still dominated by absorption bands of the neutral PAHs, which may screen the much weaker cation bands, and moreover, bands due to unknown photodegradation products may arise. PAH molecules and ions have also been studied by theoretical methods, and various density functional theory (DFT) calculations have been reported (DeFrees et al. 1993; Langhoff 1996; Bauschlicher, Hudgins, & Allamandola 1999).

Recently, we introduced a method to obtain infrared spectra of cationic PAHs through infrared multiphoton dissociation of the ions stored in a quadrupole trap (Oomens et al. 2000). The spectra of cationic naphthalene, phenanthrene, anthracene, and pyrene were recorded and show good agreement with DFT calculations and matrix isolation data. In this Letter, we present the infrared spectrum of the coronene cation, $C_{24}H_{12}^{+}$. It is (one of) the largest molecular ion(s) of which the gas-phase infrared spectrum was ever measured.

In many of the discussions on the PAH hypothesis, coronene takes a special place within the seemingly infinite group of PAHs; it is often regarded as an archetypal interstellar PAH. The highly pericondensed structure of the six fused aromatic rings results in a high thermodynamic stability, which favors its formation during PAH growth (Stein 1978; Frenklach & Feigelson 1989). Coronene is found to be relatively resistant to UV photodecomposition (Mendoza-Gomez, de Groot, & Greenberg 1995), which is of importance in view of the harsh conditions of the ISM. In the gas phase, the only fragmentation channel is hydrogen detachment from the carbon skeleton (Jochims et al. 1994; Ekern et al. 1997). From the intensity ratio of the 3.3, 3.4, and 11.3 μm UIR band features, PAHs in the size range of 20–50 carbon atoms—thus including coronene $C_{24}H_{12}$—are estimated to be responsible for the emission (Allamandola et al. 1985; Barker, Allamandola, & Tielens 1987). More recently, from the spacing between the 6.2 and 7.6 μm features, Hudgins & Allamandola (1999a) conclude that species containing 50–80 carbon atoms are the dominant emitters, although species from 20 C atoms onward also contribute significantly. Interestingly, relative line intensities in matrix isolation spectra of cationic coronene (Szczepanski & Vala 1993; Hudgins & Allamandola 1995) disagree severely with DFT-based calculations (Langhoff 1996). Finally, from a purely spectroscopic viewpoint, it should be noted that the ground electronic state of the coronene cation is degenerate, and there-

[1] FOM Institute for Plasma Physics "Rijnhuizen," Edisonbaan 14, 3439MN Nieuwegein, Netherlands; joso@rijnh.nl.
[2] General Physics Institute RAS, Vavilov Street 38, Moscow 119991, Russia.
[3] Space Research Organization of the Netherlands/Kapteyn Institute, University of Groningen, 9700AV Groningen, Netherlands.
[4] Department of Molecular and Laser Physics, University of Nijmegen, P.O. Box 9010, 6500GL Nijmegen, Netherlands.

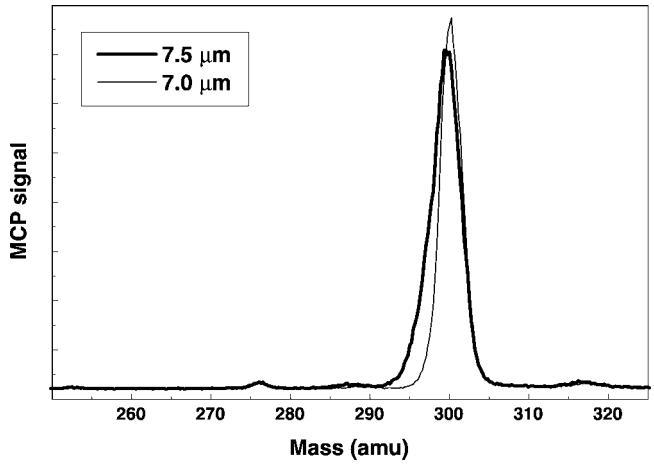

FIG. 1.—TOF traces of the coronene cation recorded with FELIX on and off the 7.5 μm infrared resonance. Although the individual H_n-loss fragments are not resolved in our mass spectrometer, the effects of multiphoton infrared dissociation are clearly observable. The small peak appearing at 276 amu is not due to coronene fragmentation but probably due to a contamination undergoing charge transfer with the coronene cations.

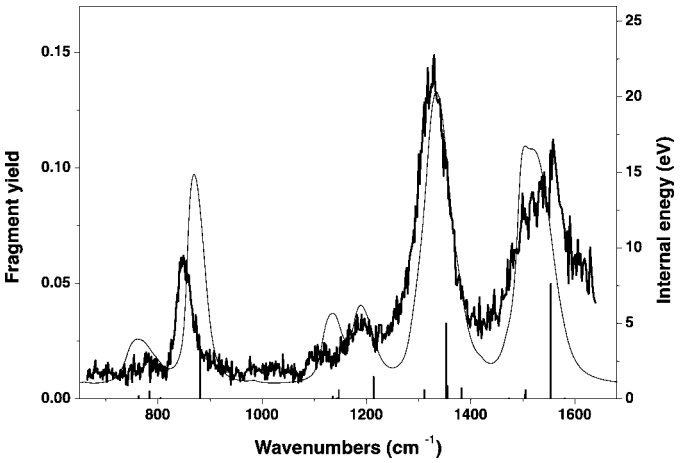

FIG. 2.—Experimental infrared multiphoton absorption spectrum of cationic coronene (*thick line, left scale*) quadratically corrected for FELIX pulse energy, compared to DFT calculations (*stick spectrum*) of Langhoff (1996) and to the calculated multiphoton absorption spectrum (*thin line, right scale*).

fore it is subject to Jahn-Teller interaction (Herzberg 1950, p. 40), which leads to an effective reduction of symmetry from D_{6h} to D_{2h} and may complicate DFT-based calculations as is, e.g., found in the case of cationic benzene (Satink et al. 1999).

The experimental technique applied here is described in detail elsewhere (Oomens et al. 2000). Briefly, coronene molecules effuse from a sample oven at about 415 K toward the center of a Paul-type quadrupole ion trap (Paul 1990), where they are ionized by the focused radiation of a KrF excimer laser. The ions are instantaneously trapped, and UV-induced fragment ions are ejected from the trap by a pulsed (2 ms) increase of the amplitude of the radio frequency voltage that is applied to the ring electrode of the trap. Subsequently, the coronene ions are irradiated with the intense and narrowband tunable infrared light generated by a free electron laser. The Free Electron Laser for Infrared eXperiments (FELIX; Oepts, van der Meer, & van Amersfoort 1995) delivers 5 μs long macropulses of light at a 10 Hz repetition rate, which consist of a 1 GHz train of micropulses. The wavelength is continuously tunable from 5 to 250 μm, and the macropulse energy can reach up to 100 mJ. The bandwidth is determined by the micropulse length (0.1–10 ps) and is typically 0.6% (FWHM) of the central wavelength in the experiments discussed here. Whenever the laser wavelength is in resonance with an allowed vibrational transition in the ion, the absorption of multiple photons can take place. FELIX pulse energies are such that more than a hundred photons can be sequentially absorbed, and thus dissociation is induced. The ions are then pulse-extracted from the trap and analyzed in a time-of-flight (TOF) mass spectrometer. Recording the fragment ion yield as a function of FELIX wavelength reveals the infrared spectrum of the parent ion against zero background.

As mentioned above, the coronene molecule/ion can withstand fairly high internal energies before decomposition occurs. In our experiments, loss of one or more hydrogen atoms are the only observed decay channels, in agreement with experiments by Jochims et al. (1994) and by Ekern et al. (1997). Typical mass spectra with FELIX on and off an infrared resonance are shown in Figure 1. Although the resolution of the trap/TOF spectrometer is insufficient to fully resolve the coronene ion from the fragments having lost one or more hydrogen atoms, the fragmentation effects are clearly observable. By recording the signal in the low-mass flank of the main peak and ratioing it to the total peak intensity, one obtains the infrared spectrum as is shown in Figure 2. Observed peak positions and intensities are listed in Table 1 along with matrix isolation data (Szczepanski & Vala 1993; Hudgins & Allamandola 1995) and DFT calculations (Langhoff 1996; C. W. Bauschlicher Jr. 2001[5]).

Due to variations in the pulse energy of FELIX as a function of wavelength, it is necessary to normalize the observed spectrum. Since the technique applied here relies on the sequential absorption of many photons by a single ion, it is not a priori clear how the signal intensity depends on applied laser power. This dependence is therefore examined by recording the peak near 7.5 μm at various laser power levels. Empirically, a near-quadratic dependence is found, as can be seen in Figure 3, and the spectrum as shown in Figure 2 was therefore normalized accordingly. Relative intensities are estimated to be correct to within $\pm 20\%$.

[5] See http://george.arc.nasa.gov:80/~cbauschl.

TABLE 1

INFRARED BANDS OF THE CORONENE CATION

CALCULATED[a]			MPD[b]		MATRIX[c]		MATRIX[d]	
D_{2h}[e]	ν_{vib}	I_{rel}[f]	ν_{vib}	I_{rel}	ν_{vib}	I_{rel}	ν_{vib}	I_{rel}
B_{2u}	784	0.07	780	0.05	…	…	…	…
B_{3u}	881	0.42	849	0.41	875	1.00	875	1.00
B_{2u}	1147	0.08	1111	0.09	…	…	…	…
B_{2u}	1213	0.20	1190	0.17	…	…	…	…
B_{2u}	1311	0.08	…	…	…	…	…	…
B_{1u}	1353	0.66	1327	1.00	1379	0.17	1379	0.34
B_{2u}	1355	0.12	…	…	…	…	…	…
B_{2u}	1382	0.10	…	…	…	…	…	…
B_{2u}	1505	0.08	…	…	…	…	…	…
B_{1u}	1553	1.00	1533	0.62	1579	0.83	…	…

[a] Langhoff 1996; C. W. Bauschlicher Jr. 2001 (see footnote 5).
[b] Multiphoton dissociation; from this work.
[c] Hudgins & Allamandola 1995.
[d] Szczepanski & Vala 1993.
[e] Symmetry lowered from D_{6h} due to Jahn-Teller distortion.
[f] Only bands with $I_{rel} > 0.06$ are listed.

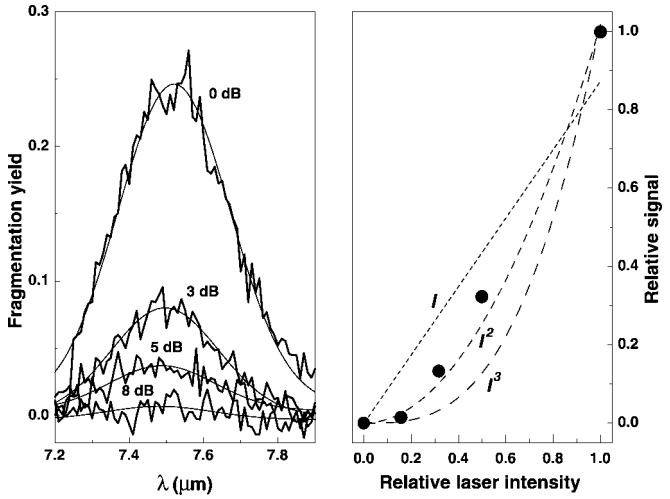

FIG. 3.—The 7.5 μm band recorded at various FELIX power levels reveals a near quadratic dependence of the signal on laser intensity. The thin lines in the left panel represent Gaussian fits of the band. The dashed lines in the right panel are linear, quadratic, and cubic power fits.

The experimental spectrum shown in Figure 2 is obtained by averaging four individual wavelength scans. All observed bands are significantly broader than 0.6% of the central wavelength (i.e., $\approx$6 cm^{-1} at $\lambda = 10$ μm), and the band shape is thus mainly determined by the molecule. There is a fairly good overall agreement between experiment and the theoretical calculations by Langhoff (1996) that are indicated by the stick spectrum in Figure 2. The CH out-of-plane bending mode is observed at 849 cm^{-1}, in the range where it is expected based on the fact that coronene possesses only aromatic rings with doubly adjacent CH bonds (Hudgins & Allamandola 1999b). The other two main absorption bands near 1327 and 1533 cm^{-1}, due to CC stretching modes, are relatively broad, which is probably caused by the presence of additional unresolved absorptions as is shown by the DFT calculations (Fig. 2, *stick spectrum*). Three weaker and semiresolved bands, observed near 780, 1111, and 1190 cm^{-1}, appear to be in good agreement with theory. All bands in the experimental spectrum are shifted to the red compared to the calculated spectrum. This shift is most likely due to vibrational anharmonicities that affect the multiphoton spectrum and is discussed below. In addition, calculations often give line positions that are shifted to the blue of the true position.

When comparing our spectrum with matrix isolation spectra (Szczepanski & Vala 1993; Hudgins & Allamandola 1995), a remarkable difference in relative intensities is immediately noticed (Table 1). In the matrix spectra, an anomalous intensity ratio between the CH out-of-plane bending mode and the CC stretching modes was found, which could not be explained. In the spectrum presented here, the 1327 cm^{-1} CC stretching mode is stronger than the CH out-of-plane bending mode, which is in agreement with the general trend for cationic PAHs. In addition, the intensity ratio between the 849 and 1327 cm^{-1} bands in our spectrum is in reasonably good agreement with the calculated spectrum (Langhoff 1996), as is seen in Figure 2. The weaker bands observed near 780, 1111, and 1190 cm^{-1} are in good agreement with the calculated spectrum but are not observed at all in the matrix isolation spectra (Szczepanski & Vala 1993; Hudgins & Allamandola 1995).

The DFT calculated spectrum obviously represents a linear absorption spectrum, whereas the observed multiphoton spectrum is affected by the effects of anharmonicity. We therefore simulated the multiphoton absorption spectrum using a model that was previously applied to calculate the infrared multiphoton ionization spectrum of neutral C_{60} (von Helden et al. 1997, 1998; van Heijnsbergen et al. 2000). The model assumes that photon absorption is followed immediately by IVR into a statistical bath of vibrational states. This assumption is justified by the huge density of vibrational states at internal energies corresponding to the oven temperature of 415 K; using the Beyer-Swineheart algorithm and the 102 normal mode frequencies reported by C. W. Bauschlicher Jr. (2001, see footnote 5), one finds a value of 10^{11} vibrational states per cm^{-1}. The rate equations describing dynamic level populations in a vibrational ladder as a function of absorption cross section, anharmonicity parameters, state density, and pump laser field are then evaluated numerically (von Helden et al. 1998). Besides calculated normal mode frequencies and intensities (C. W. Bauschlicher Jr. 2001, see footnote 5), the calculation requires anharmonicity and broadening parameters as input, which are approximated by those of the corresponding modes of neutral coronene, as reported by Joblin et al. (1995). For the weaker bands, for which no data are available, we assume averaged anharmonicity parameters. Line widths and shifts are assumed to vary linearly with internal energy.

The resulting spectrum of absorbed energy as a function of infrared frequency is plotted in Figure 2 along with the experimental trace, and a fairly good agreement is found. All bands have undergone a redshift with respect to the DFT data as a result of anharmonicity. The infrared fluence assumed in the calculation (5 J cm^{-2}) determines the amount of redshift as it determines the level of excitation that is reached (indicated on the right ordinate). The calculation shows that under realistic experimental conditions, the coronene ion reaches internal energies up to $\sim$10–20 eV. One notices that the intensity ratio between the bands at 1327 and 1533 cm^{-1} reverses with respect to the linear spectrum—in good agreement with observations. This is due to the fact that the anharmonicity for the 1533 cm^{-1} band of -0.041 cm^{-1} K^{-1} is the largest of all modes (Joblin et al. 1995). It is very interesting to note that in the PAH hypothesis, the infrared emission spectrum, which is generated after the absorption of a UV photon, originates from a molecule with some 10 eV of internal energy and is affected by the same molecular anharmonicity parameters (Barker et al. 1987; Cook & Saykally 1998), although possibly to a lesser extent depending on the level of excitation.

In Figure 4, the experimental spectrum is plotted along with an *Infrared Space Observatory* (*ISO*) Short-Wavelength Spectrometer spectrum of the photodissociation region in the Orion Bar (in the Great Orion Nebula, M42), where the degree of ionization is expected to be high (Bregman et al. 1989; Allamandola, Hudgins, & Sandford 1999; Bakes, Tielens, & Bauschlicher 2001) due to the intense radiation of the newly formed Trapezium stars. In terms of relative intensities of the CC (5–9 μm) to the CH (11–14 μm) modes, the coronene cation spectrum shows a better global agreement with the observations than the neutral coronene spectrum (*dashed line*; generated from the data of Joblin et al. 1994 taken at 770 K). Strong CC modes relative to CH modes are a general characteristic of cationic PAHs (Szczepanski & Vala 1993; Hudgins & Allamandola 1995; Langhoff 1996; Oomens et al. 2000). The comparison suggests that ionic PAHs are likely the main emitters in the 6–9 μm region, whereas both neutral and ionic PAHs contribute to the emission in the 11–14 μm range, in agreement with theoretical predictions (Langhoff 1996). In addition, as-

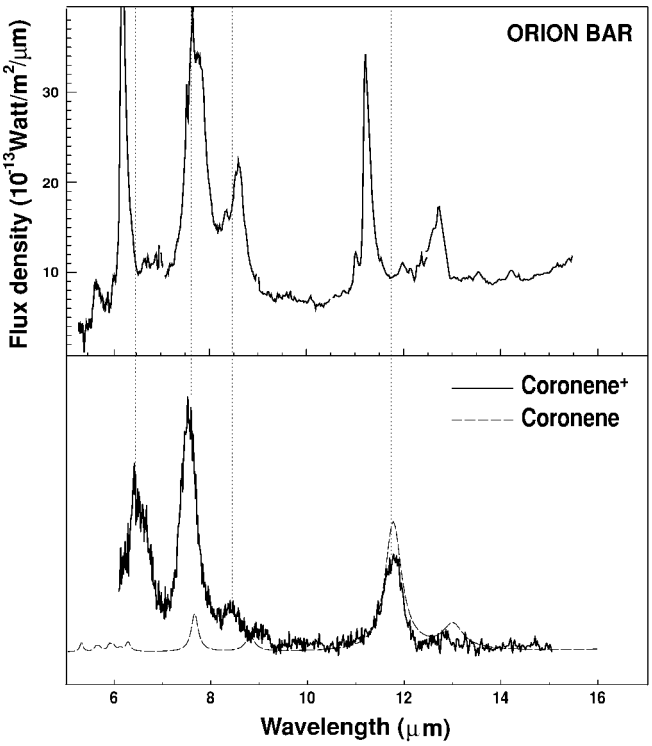

FIG. 4.—Infrared emission spectrum of the ionization region in the Orion Bar (*upper panel*) compared to the experimental spectrum of cationic coronene (*lower panel*). The dashed line indicates the gas-phase spectrum of neutral coronene at 770 K (~2 eV) of internal energy (Joblin et al. 1994).

suming that relative intensities as calculated by Langhoff (1996) are correct, as is suggested by our experiments, interstellar emission in the 3 μm range is mainly due to neutral species, since calculated 3 μm intensities for ionic PAHs are generally very low. Although the most prominent experimental band in the cation falls just within the envelope of the 7.7 μm UIR band, the feature centered at 1533 cm^{-1} is substantially redshifted compared to the 6.2 μm UIR band. It is now clear that this particular emission feature is severely blueshifted with respect to CC stretching bands of all PAHs that have been experimentally studied (E. Peeters et al. 2001, in preparation). Various theoretical studies predict a blueshift of the CC stretching modes in larger PAHs (Hudgins & Allamandola 1999a), less symmetric PAHs, nitrogen-substituted PAHs, and closed-shell ionic PAHs (Hudgins, Bauschlicher, & Allamandola 2001). On the long-wavelength side of the spectrum, the CH out-of-plane bending mode due to the duo CH groups clearly falls longward of the strong 11.2 μm feature in the UIR spectrum. Apparently, the typical blueshift of this mode upon ionization (Hudgins & Allamandola 1999b; Hony et al. 2001)—partly offset by the anharmonic redshift—is insufficient for this species to reach overlap with the 11.2 μm interstellar feature, which is most likely due to mono CH units not present in coronene. Note, however, that many objects exhibit additional weaker (unresolved) emission features longward of 11.2 μm (Witteborn et al. 1989; Hony et al. 2001), as is also seen in Figure 4.

In conclusion, the spectrum of ionic coronene as presented here resolves the problem of the anomalous intensity distribution in matrix isolation spectra, which is possibly caused by matrix effects (Joblin et al. 1994). The spectrum presented here agrees well with DFT calculations if one accounts for anharmonicity associated with highly vibrationally excited species. In our spectrum, the integrated intensity in the CC stretching and in-plane CH bending modes is approximately 4–5 times higher than in the out-of-plane CH bending region, which is in the normal range for cationic PAHs (Hudgins & Allamandola 1995). This ratio is comparable to typical UIR spectra observed toward regions where the degree of ionization is assumed to be high (Allamandola et al. 1999). These new data are anticipated to be helpful in studies that model interstellar emission spectra by synthesizing spectra of complex mixtures of PAH compounds, in which ionic coronene is often included (Roelfsema et al. 1996; Cook & Saykally 1998; Allamandola et al. 1999; Hudgins & Allamandola 1999a).

We gratefully acknowledge the expert technical support from the FELIX staff as well as from A. J. A. van Roij. We thank E. Peeters for providing the *ISO* spectrum. This work is part of the research program of FOM, which is financially supported by the Nederlandse Organisatie voor Wetenschappelijk Onderzoek (NWO).

REFERENCES

Allamandola, L. J., Hudgins, D. M., & Sandford, S. A. 1999, ApJ, 511, L115
Allamandola, L. J., Tielens, A. G. G. M., & Barker, J. R. 1985, ApJ, 290, L25
———. 1989, ApJS, 71, 733
Bakes, E., Tielens, A. G. G. M., & Bauschlicher, C. W. 2001, ApJ, 556, 501
Barker, J. R., Allamandola, L. J., & Tielens, A. G. G. M. 1987, ApJ, 315, L61
Bauschlicher, C. W., Jr., Hudgins, D. M., & Allamandola, L. J. 1999, Theor. Chem. Accounts, 103, 154
Bernstein, M. P., Sandford, S. A., Allamandola, L. J., Gillette, J. S., Clemett, S. J., & Zare, R. N. 1999, Science, 283, 1135
Bregman, J. D., Allamandola, L. J., Tielens, A. G. G. M., Geballe, T. R., & Witteborn, F. C. 1989, ApJ, 344, 791
Cernicharo, J., Heras, A. M., Tielens, A. G. G. M., Pardo, J. R., Herpin, F., Guélin, M., & Waters, L. B. F. M. 2001, ApJ, 546, L123
Cook, D. J., & Saykally, R. J. 1998, ApJ, 493, 793
DeFrees, D. J., Miller, M. D., Talbi, D., Pauzat, F., & Ellinger, Y. 1993, ApJ, 408, 530
Ekern, S. P., Marshall, A. G., Szczepanski, J., & Vala, M. 1997, ApJ, 488, L39
Frenklach, M., & Feigelson, E. D. 1989, ApJ, 341, 372
Herzberg, G. 1950, Molecular Spectra and Molecular Structure, Vol. III: Electronic Spectra and Electronic Structure of Polyatomic Molecules (Malabar: Krieger)
Hony, S., Van Kerckhoven, C., Peeters, E., Tielens, A. G. G. M., Hudgins, D. M., & Allamandola, L. J. 2001, A&A, 370, 1030
Hudgins, D. M., & Allamandola, L. J. 1995, J. Phys. Chem., 99, 3033
———. 1999a, ApJ, 513, L69
———. 1999b, ApJ, 516, L41
Hudgins, D. M., Bauschlicher, C. W., Jr., & Allamandola, L. J. 2001, Spectrochim. Acta, 57, 907
Hudgins, D. M., Sandford, S. A., & Allamandola, L. J. 1994, J. Phys. Chem., 98, 4243
Joblin, C., d'Hendecourt, L., Léger, A., & Défourneau, D. 1994, A&A, 281, 923
Joblin, C., Léger, A., d'Hendecourt, L., & Défourneau, D. 1995, A&A, 299, 835
Joblin, C., Tielens, A. G. G. M., Geballe, T. R., & Wooden, D. H. 1996, ApJ, 460, L119
Jochims, H. W., Rühl, E., Baumgärtel, H., Tobita, S., & Leach, S. 1994, ApJ, 420, 307
Langhoff, S. R. 1996, J. Phys. Chem., 100, 2819
Leger, A., & Puget, J. L. 1984, A&A, 137, L5
Mendoza-Gomez, C. X., de Groot, M. S., & Greenberg, J. M. 1995, A&A, 295, 479
Oepts, D., van der Meer, A. F. G., & van Amersfoort, P. W. 1995, Infrared Phys., 36, 297

Oomens, J., van Roij, A. J. A., Meijer, G., & von Helden, G. 2000, ApJ, 542, 404
Paul, W. 1990, Rev. Mod. Phys., 62, 531
Roelfsema, P. R., et al. 1996, A&A, 315, L289
Salama, F., Bakes, E. L. O., Allamandola, L. J., & Tielens, A. G. G. M. 1996, ApJ, 458, 621
Satink, R. G., Piest, H., von Helden, G., & Meijer, G. 1999, J. Chem. Phys., 111, 10,750
Sloan, G. C., Hayward, T. L., Allamandola, L. J., Bregman, J. D., DeVito, B., & Hudgins, D. M. 1999, ApJ, 513, L65
Stein, S. E. 1978, J. Phys. Chem., 82, 566
Szczepanski, J., Roser, D., Personette, W., Eyring, M., Pellow, R., & Vala, M. 1992, J. Phys. Chem., 96, 7876
Szczepanski, J., & Vala, M. 1993, ApJ, 414, 646
van Heijnsbergen, D., von Helden, G., Sartakov, B., & Meijer, G. 2000, Chem. Phys. Lett., 321, 508
von Helden, G., Holleman, I., Knippels, G. M. H., van der Meer, A. F. G., & Meijer, G. 1997, Phys. Rev. Lett., 79, 5234
von Helden, G., Holleman, I., Meijer, G., & Sartakov, B. 1998, Opt. Exp., 4, 46
Witteborn, F. C., Sandford, S. A., Bregman, J. D., Allamandola, L. J., Cohen, M., Wooden, D. H., & Graps, A. L. 1989, ApJ, 341, 270